Biochimica et Biophysica Acta 1828 (2013) 776–784

Contents lists available at SciVerse ScienceDirect

Biochimica et Biophysica Acta

journal homepage: www.elsevier.com/locate/bbamem

Lipid–protein nanodiscs promote *in vitro* folding of transmembrane domains of multi-helical and multimeric membrane proteins

Zakhar O. Shenkarev [a,*], Ekaterina N. Lyukmanova [a], Ivan O. Butenko [a,c], Lada E. Petrovskaya [a], Alexander S. Paramonov [a], Mikhail A. Shulepko [a], Oksana V. Nekrasova [a], Mikhail P. Kirpichnikov [a,b], Alexander S. Arseniev [a,c,*]

[a] *Shemyakin–Ovchinnikov Institute of Bioorganic Chemistry, Russian Academy of Sciences, str. Miklukho-Maklaya 16/10, Moscow, 117997 Russian Federation*
[b] *Lomonosov Moscow State University, Moscow, 119991, Russian Federation*
[c] *Moscow Institute of Physics and Technology (State University), Department of Physicochemical Biology and Biotechnology, Institutskii per., 9, 141700 Dolgoprudny, Moscow Region, Russia*

ARTICLE INFO

Article history:
Received 9 April 2012
Received in revised form 4 November 2012
Accepted 6 November 2012
Available online 13 November 2012

Keywords:
Bacteriorhodopsin ESR
Potassium channel KcsA
Reconstructed high-density lipoprotein
Membrane protein folding
Membrane mimetic
Cell-free expression

ABSTRACT

Production of helical integral membrane proteins (IMPs) in a folded state is a necessary prerequisite for their functional and structural studies. In many cases large-scale expression of IMPs in cell-based and cell-free systems results in misfolded proteins, which should be refolded *in vitro*. Here using examples of the bacteriorhodopsin ESR from *Exiguobacterium sibiricum* and full-length homotetrameric K^+ channel KcsA from *Streptomyces lividans* we found that the efficient *in vitro* folding of the transmembrane domains of the polytopic and multimeric IMPs could be achieved during the protein encapsulation into the reconstructed high-density lipoprotein particles, also known as lipid–protein nanodiscs. In this case the self-assembly of the IMP/nanodisc complexes from a mixture containing apolipoprotein, lipids and the partially denatured protein solubilized in a harsh detergent induces the folding of the transmembrane domains. The obtained folding yields showed significant dependence on the properties of lipids used for nanodisc formation. The largest recovery of the spectroscopically active ESR (~60%) from the sodium dodecyl sulfate (SDS) was achieved in the nanodiscs containing anionic saturated lipid 1,2-dimyristoyl-sn-glycero-3-phosphocholine (DMPG) and was approximately twice lower in the zwitterionic DMPC lipid. The reassembly of tetrameric KcsA from the acid-dissociated monomer solubilized in SDS was the most efficient (~80%) in the nanodiscs containing zwitterionic unsaturated lipid 1-palmitoyl-2-oleoyl-sn-glycero-3-phosphocholine (POPC). The charged and saturated lipids provided lower tetramer quantities, and the lowest yield (<20%) was observed in DMPC. The overall yield of the ESR and KcsA folding was mainly restricted by the efficiency of the protein encapsulation into the nanodiscs.

1. Introduction

Helical integral membrane proteins (IMPs) play key roles in a variety of biological processes essential for living cells and multicellular organisms [1]. About one quarter of the human genes are predicted to encode for IMPs [2] and more than 50% of current pharmaceutical drugs target membrane proteins [3]. In spite of the large interest in this field, the molecular mechanisms of IMP functioning are not very well established. The difficulties in functional and structural studies of IMPs are conditioned by the requirement of a biological membrane or suitable membrane mimicking medium (membrane mimetic) which should support a native spatial structure and functional activity of the proteins.

One of the main problems that hinder structure-functional IMP investigations is the production of milligram quantities of the natively folded proteins in a state with a sufficient life-time and thermal stability [4,5]. Membrane targeted expression in bacterial, yeast, insect or mammalian cells is traditionally used for the production of the functionally active IMPs [4,5], although the high-level heterologous expression within the cellular membranes was reported only in a limited number of cases [1,4,5]. Large-scale production of IMPs in a misfolded form (e.g. in a form of insoluble bacterial inclusion bodies) followed by the *in vitro* folding represents a promising alternative to the membrane targeted expression [6,7]. Recently cell-free (CF) systems attract much attention as an alternative tool for the high-level recombinant production of IMPs [8]. During CF synthesis milligram quantities of a membrane protein could be produced either in a form of insoluble reaction

Abbreviations: CF, cell-free; DDM, n-dodecyl-β-D-maltopyranoside; DMPC, 1,2-dimyristoyl-sn-glycero-3-phosphocholine; DMPG, 1,2-dimyristoyl-sn-glycero-3-phosphoglycerol; DOPG, 1,2-dioleoyl-sn-glycero-3-phosphoglycerol; DOPE, 1,2-dioleoyl-sn-glycero-3-phosphoethanolamine; ESR, bacteriorhodopsin from *Exiguobacterium sibiricum*; IMP, integral membrane protein; KcsA, K^+-channel from *Streptomyces lividans*; LPN, lipid–protein nanodisc; mKcsA, monomeric form of KcsA; MSP, membrane scaffold protein; MSP^+, MSP with the *N*-terminal His_6-tag sequence; MSP^-, MSP without His_6-tag; POPC, 1-palmitoyl-2-oleoyl-sn-glycero-3-phosphocholine; R_{St}, hydrodynamic radius of a particle, Stokes radius; SEC, size exclusion chromatography; SDS, sodium dodecyl sulfate; tKcsA, tetrameric form of KcsA; TM, transmembrane

* Corresponding authors at: str. Miklukho-Maklaya, 16/10, Moscow, 117997, Russian Federation. Tel.: +7 495 330 74 83.
E-mail addresses: zh@nmr.ru (Z.O. Shenkarev), aars@nmr.ru (A.S. Arseniev).

0005-2736/$ – see front matter © 2012 Elsevier B.V. All rights reserved.
http://dx.doi.org/10.1016/j.bbamem.2012.11.005

mixture precipitate or in a soluble form in the presence of membrane mimetics [8]. In spite of the ability to produce soluble IMPs, in some cases the CF synthesis results in a misfolded protein and requires an application of the refolding procedure [9].

In general the problem of the *in vitro* IMP folding could be subdivided into the two interconnected tasks: the folding of extramembrane domain(s) and folding of a transmembrane (TM) domain. The last task is probably more challenging, as the universal and generally applicable protocols for the *in vitro* folding of the IMPs containing multi-helical (polytopic) TM domains are presently unavailable [10,11]. Successful examples usually involve several steps [6,7,12]. Initially a misfolded and aggregated protein is solubilized in a harsh detergent or organic solvent with possible addition of chaotropic agents. This step results in the formation of the monomeric protein with the partially or completely formed secondary structure (helices) and unformed or nascent tertiary structure (partially denatured protein state) [13]. The folding is accomplished by a transfer of the solubilized protein into the appropriate membrane mimicking medium able to support the correct IMP spatial structure [14]. Micelles of mild detergents [15], lipid/detergent mixtures (bicelles) [16], lipid vesicles [17,18], or synthetic surfactants (amphipols) [7] are generally used for this purpose.

In the present report we showed the successful application of an alternative membrane mimicking medium - lipid-protein nanodiscs (LPNs), for the *in vitro* folding of recombinant helical IMPs. The LPNs, also known as reconstructed high-density lipoprotein particles, encapsulate a patch of lipid bilayer (~10 × 4 nm, ~150 lipids) stabilized in a solution by two copies of either apolipoprotein or special membrane scaffold protein (MSP) [19]. It has been shown by the numerous examples that IMPs obtained by the membrane-targeted expression in a folded state and subsequently extracted under non-denaturing conditions by mild detergents can be reconstructed into the LPNs without loss in the functional activity [20,21]. Moreover the obtained IMP/LPN complexes provide the long-term stability for the encapsulated proteins [20,21]. Here we demonstrated that the *in vitro* folding of the TM domains of the polytopic or multimeric helical IMPs could be achieved during the self-assembly of the IMP/LPN complexes starting from the partially denatured IMPs solubilized in a harsh detergent (Fig. 1). Utility of the proposed approach was verified using the bacteriorhodopsin from *Exiguobacterium sibiricum* (ESR, 7 TM helices) and homotetrameric full-length K^+ channel KcsA from *Streptomyces lividans* (2 TM helices per subunit). Obtained results revealed that the lipid composition of LPNs represents one of the key determinants of the efficient IMP folding.

2. Materials and methods

2.1. Materials

SDS was a product of Sigma (St. Louis, MO). Sodium cholate and DDM were products of Anatrace Inc. (Maumee, OH). All used lipids (DMPC, DMPG, DOPG, DOPE, POPC) were products of Avanti Polar Lipids (Alabaster, AL). Two variants of the membrane binding domain (44–243 fragment) of human apolipoprotein A-I with the *N*-terminal His_6-tag sequence (MSP^+, 26.0 kDa) and without His_6-tag (MSP^-, 23.3 kDa) were produced as described in [22]. Concentrations of the MSP^+ and MSP^- were measured using UV absorbance at 280 nm (molar extinction coefficients 26.93 and 23.95 $mM^{-1} \cdot sm^{-1}$, respectively).

2.2. Reconstitution of the ESR/LPN complexes

ESR with the *C*-terminal His_6-tag sequence (28.8 kDa) was either expressed in *E. coli* membranes as described in [23] or synthesized as a precipitate using the continuous exchange CF system [8] in the absence of any membrane mimicking components as described in [9]. In the first case the protein was extracted from the bacterial membranes by 1% DDM, purified on Ni^{2+}-Sepharose 6 Fast Flow column (GE Healthcare), and precipitated by the addition of 10% cold (−20 °C) trichloroacetic acid. The precipitate was three times extensively washed with cold acetone (−20 °C) to remove the DDM traces and dried on the air. In the second case the insoluble fraction of the CF reaction mixture containing synthesized ESR was separated by centrifugation for 15 min, at 14,000 rpm. In both cases the precipitated protein was solubilized in buffer A (20 mM Tris/HCl, 250 mM NaCl, 1 mM NaN_3, pH 8.0) containing 2% SDS. ESR/SDS sample (47 μM, 0.17 ml) was mixed with MSP^-, all-*trans* retinal, and lipids (DMPC or DMPG) at a 1:30:4:1800 molar ratio without the addition of sodium cholate. The final reaction volume was 2.0 ml, the ESR concentration was 4.0 μM, and the SDS concentration was adjusted to 0.5%. The final ESR/SDS molar ratio was ~1:4300. The mixture was incubated overnight at 25 °C with gentle

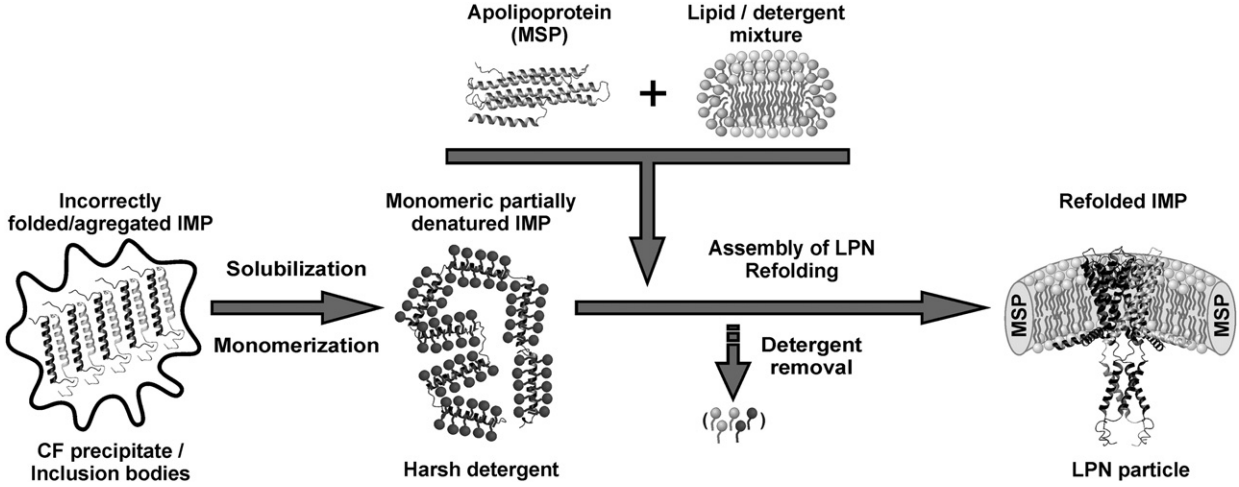

Fig. 1. Scheme illustrating the proposed approach for the *in vitro* folding of recombinant helical IMPs. The ribbon representation of MSP and IMP molecules is shown using the examples of human apolipoprotein A-I and KcsA (PDB ID: 2A01 and 1F6G, respectively). For homotetrameric KcsA one subunit is shown in gray and others in black. Lipid molecules are drawn in light gray and detergent molecules in dark gray and black. Two MSP molecules stabilizing the membrane fragment of the nanodisc are drawn as a torus. Please note that the initial structural state of an aggregated/misfolded helical IMP could depend on the employed method of the recombinant production. Precipitate of CF system (schematically shown on the left) probably contains an IMP with the significant level of the already formed helical secondary structure. At the same time the bacterial inclusion bodies could contain the strongly aggregated proteins with the β-sheet-rich amyloid-like structure.

shaking. Reconstruction of the ESR/LPN complexes was initiated by the incubation with 0.5 g of Biobeads™ (BioRad, Hercules, CA) per 1 ml of the reaction during 2 h at 25 °C and gentle shaking. The ESR/LPN complexes were purified on Ni^{2+}-column equilibrated in buffer A. The column was washed with ten volumes of buffer A and fractions with ESR/LPNs were eluted with buffer A containing 100 mM imidazole, dialyzed against buffer B (10 mM Tris/acetate, 10 mM EDTA, and 1 mM NaN_3, pH 7.0), and concentrated using Stirred Cells with Ultrafiltration Membranes, NMWL 10,000 (Millipore, Billerica, MA).

To prepare the ESR/LPN complexes for a control experiment, the spectroscopically active protein was extracted from *E. coli* membranes in the presence of all-*trans*-retinal and purified in the presence of 0.2% DDM as described in [23]. ESR/DDM sample (66 μM, 0.45 ml) was mixed in buffer A with MSP^-, DMPG, and sodium cholate at a 1:20:1600:3200 molar ratio. The final reaction volume was 5.0 ml, the ESR concentration was 6.0 μM, and the ESR/DDM molar ratio was ~1:60. The assembly and purification of the ESR/LPN complexes were done using the protocol described above.

2.3. Reconstitution of the KcsA/LPN complexes

KcsA channel (homotetramer of 18.5 kDa subunits) was expressed in *E. coli* membranes, extracted by 1% DDM, and purified by Ni^{2+}-affinity chromatography using *C*-terminal His_6-tag as described in [24,25]. KcsA was precipitated from DDM by the addition of 10% cold trichloroacetic acid, and washed with cold acetone as described above for ESR. The precipitate was resolubilized in buffer A containing 1% SDS. KcsA/SDS sample (70 μM, 0.15 ml, all the concentrations are given for monomeric KcsA, mKcsA) was mixed with MSP^-, lipids (DOPE/DOPG 7:3, POPC, POPC/DOPG 7:3, DMPC, or DMPG) and sodium cholate at a 1:20:800:1600 molar ratio. The final reaction volume was 0.45 ml, the mKcsA concentration was 23 μM, and the mKcsA/SDS molar ratio was ~1:500. The assembly of the KcsA/LPN complexes was done using the protocol described above for the ESR/LPN complexes. The KcsA/LPN complexes were purified on a Ni^{2+}-column equilibrated in buffer A. The column was subsequently washed with six volumes of buffer A and 4 volumes of buffer A containing 100 mM imidazole. Fractions with the KcsA/LPNs were eluted with buffer A containing 500 mM imidazole. Formation of KcsA monomers (mKcsA) and KcsA tetramers (tKcsA) was monitored by SDS-PAGE as described in [18,24]. In some of the experiments 10 mM KCl was added to all the buffers used for LPN assembly and Ni^{2+}-affinity purification.

2.4. Reconstitution of the "empty" LPNs

MSP^+ was mixed in buffer A with the lipids (POPC or DMPC) and sodium cholate at a 1:75:150 molar ratio. The final reaction volume was 0.45 ml, the MSP^+ concentration was 0.25 mM. In some of the experiments SDS was added to the reaction mixture up to the final concentration of 11.5 mM (SDS/lipid/cholate molar ratio of ~5:8:16). The assembly of the "empty" LPNs was done using the protocol described above for the ESR/LPN complexes. The LPNs were purified on Ni^{2+}-column equilibrated in buffer A. The column was washed with six volumes of buffer A and fractions with LPNs were eluted with buffer A containing 100 mM imidazole and concentrated.

2.5. Analysis of the IMP/detergent complexes, "empty" LPNs, and IMP/LPNs

The concentrations of purified ESR and mKcsA in detergent solutions were calculated from the UV absorbance at 280 nm using the molar extinction coefficients of 46.87 and 34.95 $mM^{-1} \cdot sm^{-1}$, respectively. The obtained IMP/LPN complexes were analyzed by 12% Tris/tricine SDS-PAGE. Each SDS-PAGE gel was supplemented with a "reference" lane(s) containing the IMP/detergent complex(es) of the known concentration. The quantities of encapsulated mKcsA and tKcsA were estimated using relative intensities of the bands on Coomassie-stained SDS-PAGE gels. SDS-PAGE mobilities of ESR and MSP^- were quite similar and the bands of these proteins were indistinguishable. The quantity of encapsulated ESR was estimated by Western blot using His-tag monoclonal antibodies (Merck, Darmstadt, Germany). The blots and Coomassie-stained gels were analyzed by densitometry using OptiQuant 3.00 software (Packard Instrument Company).

The concentration of active ESR was estimated from the UV–vis absorbance at 534 nm using the molar extinction coefficient of 43.0 $mM^{-1} \cdot sm^{-1}$. This coefficient was measured for the protein extracted from *E. coli* membranes by DDM in the presence of all-*trans*-retinal (Fig. 2A). UV–vis spectra were acquired in the range from 210 to 700 nm using a Cary-50 instrument (Varian). The spectra were fitted to the sum of four Gaussian lines centered at ~210, 280, 390, and 530 nm using the program Mathematica (Wolfram Research). Rayleigh scattering contribution was accounted using an additional variable parameter. CD spectra were measured on a Jasco J-810 instrument (Jasco, Japan) at ambient temperature.

The IMP/LPN complexes and "empty" LPNs were analyzed by size-exclusion chromatography (SEC) performed on the Superdex-200, Tricorn 5/200 column (GE Healthcare) loaded into 20 mM Tris/HCl, 100 mM NaCl, 1 mM EDTA, and 1 mM NaN_3, pH 7.4. The elution rate was 0.15 ml/min, the wave length of detection was 280 nm. The sample volumes didn't exceed 30 μl, i.e. 0.77% of the total column volume. Dextran 2000, thiroglobulin (MW 669 kDa, hydrodynamic Stokes radius (R_{St}) 85 Å), ferritin (MW 440 kDa, R_{St} 61 Å), catalase (MW 232 kDa, R_{St} 52.2 Å), aldolase (MW 158 kDa, R_{St} 48.1 Å), BSA (MW 67 kDa, R_{St} 35.5 Å), and ovalbumin (MW 43 kDa, R_{St} 30.5 Å) from high and low weight calibration kits (GE Healthcare) were used for a calibration. The measured elution volumes were converted to the R_{St} values via the linear calibration graph (elution volume versus $Log(R_{St})$).

1D ^1H and 2D ^1H-^{13}C HSQC NMR spectra were measured at 45 °C on a Bruker AVANCE-III 800 spectrometer equipped with a triple-resonance cryoprobe.

3. Results

3.1. Partial unfolding of the bacteriorhodopsin ESR in the harsh detergent SDS

The light-driven proton pump of bacteriorhodopsin from *Exiguobacterium sibiricum* is composed from 7 TM helices [23] and could be considered as a structural prototype of G-protein coupled receptors (GPCRs), the ones of the most important pharmacological targets [3,4]. The activity of ESR can be easily monitored by UV–vis spectroscopy using the characteristic absorbance at 534 nm or by a visual observation of the purple color of the sample. In the present work ESR was produced either by CF synthesis in the form of the insoluble precipitate of the reaction mixture or by the *E. coli* membrane-targeted expression. In the last case the protein was extracted by 1% DDM and precipitated by trichloroacetic acid. In both cases the precipitated protein was solubilized in the harsh detergent SDS resulting in the partially denatured IMP lacking the native-like tertiary structure and altered secondary structure.

The unfolding of ESR in the presence of SDS is supported by the following observations. (1) The titration of the ESR/SDS sample by the co-factor all-*trans*-retinal did not reveal the functionally active protein (data not shown). (2) The excess of SDS added to the sample of spectroscopically active ESR solubilized in DDM led to the fast (characteristic time <60 s) disruption of the retinal binding pocket associated with the movement of the retinal absorption band from 534 to 440 nm (Fig. 2B). This process was followed by the relatively slow (characteristic time ~$2.2 \cdot 10^3$ s) dissociation of the retinal coincident with the emergence of the free retinal band at 390 nm (Fig. 2BF). (3) CD spectroscopy of ESR in the SDS solution revealed the changes in the protein secondary structure (Fig 2G). The moderate decrease in the helical content was observed. In this case the percentage of secondary structure present as α-helix, β-sheet, β-turn, and random coil, respectively, was 52%, 7%, 15%, and 25%. These values should be compared with the secondary

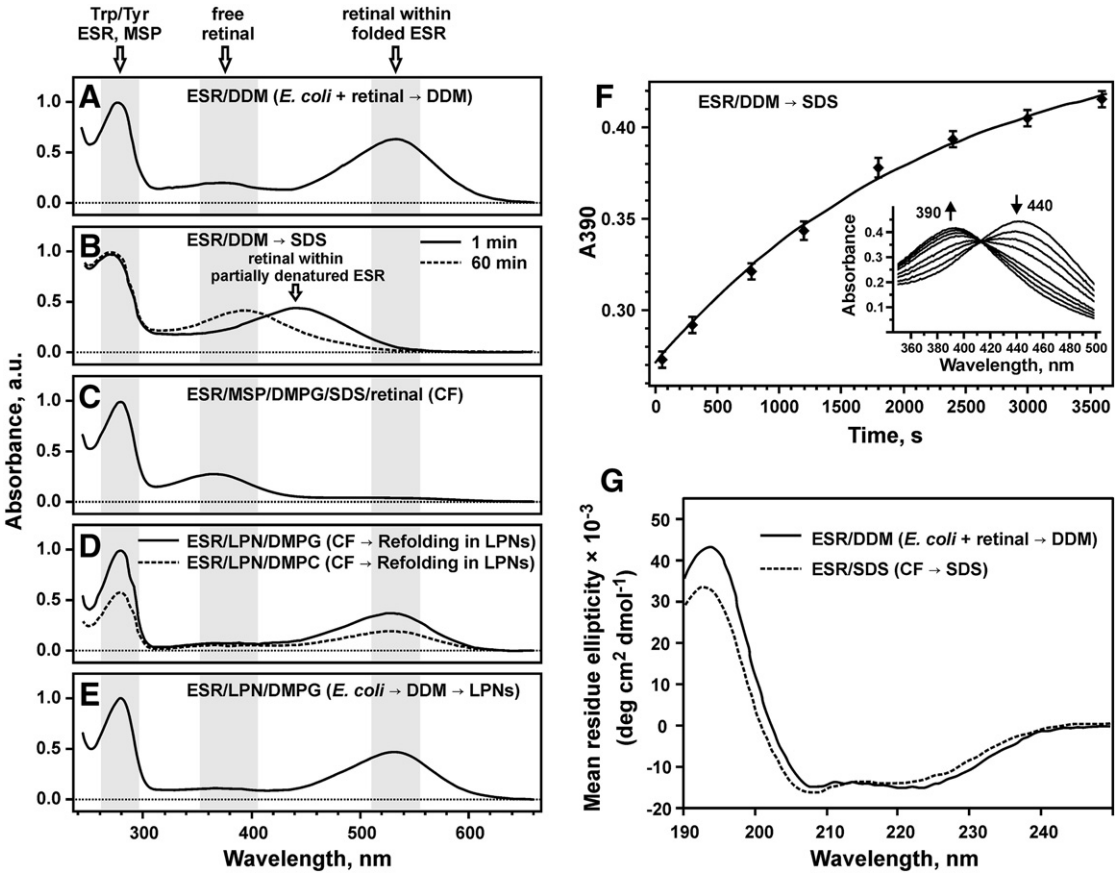

Fig 2. Light-adapted UV–vis and CD spectra of the different ESR preparations. (A). Natively folded (spectroscopically active) ESR extracted from *E. coli* membranes in 0.2% DDM. (B). Changes in ESR spectra over time on addition of 10% SDS to the protein solubilized in 0.2% DDM. After fast shift of the retinal absorbance to 440 nm (solid line; recorded at 1 min) the signal decays to a band at 390 nm corresponding to the free retinal (dashed line; recorded at 60 min). The 440 nm band is assigned to the retinal bound to the partially denatured ESR (ESR_{440}) using the data presented in [26]. The kinetic of the retinal dissociation is shown on the panel (F). Free retinal (A_{390}) is formed from ESR_{440} by a single exponential phase at 4.5×10^{-4} s^{-1}. The corresponding fragments of the UV–vis spectra are shown in the inset. The transition occurs with a single isobestic point at 413 nm. (C). ESR/MSP/DMPG/SDS/retinal mixture before the assembly of the nanodiscs. (D) Purified ESR/LPN/DMPG (solid line) and ESR/LPN/DMPC (dashed line) complexes containing the active bacteriorhodopsin refolded using equal starting amounts of the protein. (E) Purified ESR/LPN/DMPG complexes reconstructed using the active bacteriorhodopsin extracted from *E. coli* membranes by DDM. All spectra were measured at pH ~ 8.0. The spectra are scaled relative to the "aromatic" band at 280 nm. The relative scaling of spectra in the panel (D) is preserved. (G) CD spectra of natively folded ESR extracted from *E. coli* membranes in 0.2% DDM (solid line) and partially unfolded ESR solubilized from the CF precipitate by 2% SDS (dashed line).

structure composition of spectroscopically active ESR solubilized in DDM (66%, 5%, 10%, and 19%, respectively, Fig. 2G). The similar partial IMP denaturation characterized by the fast disruption of the retinal binding pocket, slow dissociation of retinal (absorbance transition from 440 to 390 nm), and decrease in the helical content from 78% to 53% was previously observed for the *H. salinarum* bacteriorhodopsin in the SDS solution [26]. Recently, the detailed structural description of the partially denatured *H. salinarum* bacteriorhodopsin was obtained by EPR spectroscopy [13]. The almost complete disruption of the tertiary interhelical contacts was observed upon the protein solubilization in SDS [13].

3.2. In vitro folding of the bacteriorhodopsin ESR

According to the published data the mixtures of lipids with the CHAPS detergent are able to induce the *in vitro* folding of the *H. salinarum* bacteriorhodopsin from the SDS denatured state [14,16,27]. Sodium cholate, the detergent commonly used for the nanodisc assembly [20,21], is structurally related to CHAPS and also could promote the bacteriorhodopsin folding. Indeed, the addition of the DMPC/cholate/retinal mixture to the ESR/SDS sample induced the spontaneous folding of the protein (data not shown). To investigate the bacteriorhodopsin folding during the LPN reconstruction, the nanodisc self-assembly protocol was modified. ESR/LPN complexes were assembled from the mixture of the protein with SDS, MSP^{-}, and differently charged saturated lipids (DMPC or DMPG) without the addition of sodium cholate. In this case SDS (0.5%) was the only detergent component of the reaction. The titration of the above mixtures by all-*trans*-retinal did not reveal the active protein (Fig. 2C) indicating that the addition of lipids and MSP^{-} does not induce the folding of ESR from the SDS denatured state. It should be mentioned that the unsaturated lipids (POPC, DOPG) were not tested for the ESR folding due to their low solubility in SDS. The mixtures of POPC or POPC/DOPG with MSP^{-} and SDS remained turbid even after the vigorous sonication.

The self-assembly of the nanodiscs and simultaneous ESR folding were initiated by removing the detergent (SDS) by the Biobeads™ adsorbent. The assembled ESR/LPN/DMPC and ESR/LPN/DMPG complexes were purified by Ni^{2+}-affinity chromatography using His_6-tag at the ESR molecule. In both cases the predominant formation of the particles with the diameter expected for the nanodiscs (~10 nm) were observed by SEC (Fig. 3A, traces 1 and 2, respectively). According to the data of UV–vis spectroscopy (Fig. 2D) both types of LPNs contained the folded (spectroscopically active) bacteriorhodopsin. The total amount of ESR encapsulated into the nanodiscs and the amount of active ESR were estimated by Western blot and UV–vis spectroscopy, respectively. The comparison of these values with the protein amount initially used for

the nanodisc assembly revealed that the overall yields of the refolding process were about 30% (DMPC) and 60% (DMPG). The variation in the yields mostly arose from the efficiency of the ESR reconstruction into different LPNs (~40% and 75% in the case of DMPC and DMPG, respectively). In contrast to that, the efficiency of the ESR folding inside the nanodiscs (the concentration ratio of the spectroscopically active protein to the total amount of the nanodisc encapsulated bacteriorhodopsin) in both cases was quite similar (~80%). The approximately same yields of the refolding (±5%) were obtained for both CF synthesized ESR and the protein expressed in *E. coli*.

The fact that the overall yield of the ESR folding was restricted by the efficiency of the protein reconstruction into LPNs could be illustrated by the direct comparison of UV–vis spectra of the obtained ESR/LPN/DMPC and ESR/LPN/DMPG complexes (Fig. 2D). For both preparations the ratio of intensities of the spectral bands at 534 and 280 nm was equal to ~0.35. This, assuming a 2:1 MSP/ESR stoichiometry of the ESR/LPN complexes (i.e. one ESR molecule per nanodisc), permitted the estimation of the content of the active bacteriorhodopsin in the samples as about 80%. At the same time the overall intensity of the ESR/LPN/DMPC spectrum was almost twice lower, indicating lower efficiency of the ESR/LPN reconstruction in this case. Interestingly, the ratio of intensities of the spectral bands at 534 and 280 nm for the ESR/LPN/DMPG complexes reconstructed using the folded protein solubilized in DDM (Fig. 2E) was equal to ~0.47, which was quite close to the value (0.46) expected for 2:1 MSP/ESR stoichiometry.

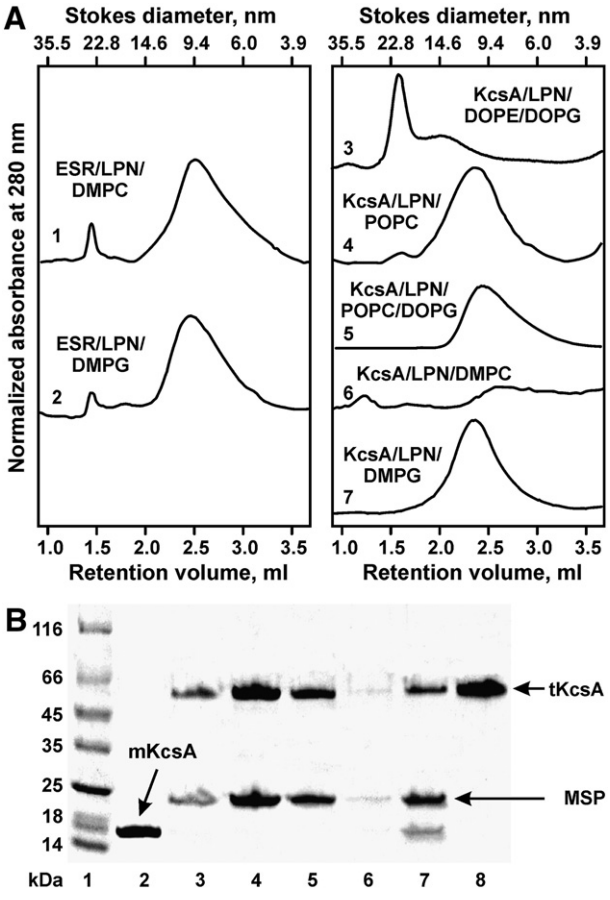

Fig 3. SEC (A) and SDS-PAGE (B) analysis of the ESR/LPN and KcsA/LPN preparations after Ni^{2+}-affinity purification. The KcsA/LPN complexes were assembled and purified in the presence of 10 mM KCl. (A) 1—ESR/LPN/DMPC; 2—ESR/LPN/DMPG. 3—KcsA/LPN/DOPE/DOPG; 4—KcsA/LPN/POPC; 5—KcsA/LPN/POPC/DOPG; 6—KcsA/LPN/DMPC; 7—KcsA/LPN/DMPG; (B) 1—molecular mass markers; 2—monomeric form of KcsA (mKcsA) in SDS; 3—KcsA/LPN/DOPE/DOPG; 4—KcsA/LPN/POPC; 5—KcsA/LPN/POPC/DOPG; 6—KcsA/LPN/DMPC; 7—KcsA/LPN/DMPG; 8—tetrameric form of KcsA (tKcsA) in DDM.

3.3. In vitro folding of the K^+ channel KcsA

To show the applicability of the proposed method to the folding of multimeric proteins we used the full-length K^+-channel KcsA. According to the published crystal structures [28,29] and the results of NMR [30,31] and EPR investigations [32], KcsA is composed of the four identical subunits, which surround the channel pore (see Fig 1). Each subunit includes *N*- and *C*-terminal helical domains exposed to a solvent and a membrane-associated domain composed of two TM helices with a P-loop between them. The oligomeric state of KcsA can be easily monitored by SDS-PAGE [18,24]. The natively folded channel extracted from *E. coli* membranes by the mild detergents preserved its tetrameric organization (tKcsA) even in the SDS solution [30]. At the same time the dissociated mKcsA monomers could not spontaneously form homotetramers in the SDS environment. The recent NMR study of SDS solubilized mKcsA revealed the partially denatured protein with the distorted tertiary and secondary structures [33].

SDS-PAGE analysis (Fig 3B, lane 8 and Fig. S1, lane 11) revealed that KcsA extracted from *E. coli* membranes by the mild detergent DDM (1%) preserved its tetrameric organization (tKcsA). After extraction the protein was precipitated by trichloroacetic acid and resolubilized in SDS. This procedure led to the tKcsA denaturation and formation of monomeric mKcsA (Fig 3B, lane 2). To achieve the refolding of the channel tetramer, the KcsA/LPN complexes were reconstructed from the partially denatured mKcsA solubilized in SDS using the conventional protocol of the nanodisc assembly [20,21]. Influence of the lipid properties on the tKcsA folding was studied with the differently charged unsaturated (DOPE/DOPG 7:3, POPC, POPC/DOPG 7:3) and saturated (DMPC, DMPG) lipids. The two sets of the experiments were conducted: (1) with addition of 10 mM KCl in the buffers used for the nanodisc assembly and Ni^{2+}-affinity purification (Fig. 3B) and (2) without explicit addition of potassium ions (Fig. S1 and S2). In all the tested cases the removal of detergents (SDS and sodium cholate) led to the tetramer formation. The efficiency of the tKcsA folding markedly depended on the properties of the used lipids and the residual content of mKcsA was detected in some of the experiments (e.g. Fig. 3B, lane 7, Fig. S1). The Ni^{2+}-affinity co-purification of the MSP^- molecules with the tetramers of His_6-tagged KcsA confirmed the formation of the tKcsA/MSP^- complexes in all the tested cases (Fig S1 and S2). At the same time SEC analysis revealed the successful formation of nanodiscs with the expected diameter (~10 nm) only in three of the five used lipid compositions (POPC, POPC/DOPG, DMPG, Fig. 3A, traces 4, 5, and 7).

Densitometry analysis of the Coomassie-stained SDS-PAGE gels (Fig. 3B and S1) provided the rough estimates of the yields of refolded tKcsA and the residual fraction of mKcsA (Table 1). The measured yields of the tKcsA refolding within the experimental error did not depend on the explicit addition of potassium ions. At the same time the relative content of mKcsA was lower in the nanodisc preparations assembled in the presence of 10 mM KCl (Table 1). The largest efficiency of the *in vitro* tKcsA folding (~80%) was observed in LPNs containing POPC (Fig. 3B, lane 4, Fig. 1S, lane 4). (The given value represents the average of two experiments: with and without 10 mM KCl, see Table 1) The addition of the negatively charged lipids into this system (POPC/DOPG 7:3) diminished the yield of nanodisc encapsulated tKcsA to ~55% (Fig. 3B, lane 5, Fig. 1S, lane 6). The replacement of the phosphatidylcholine lipid by phosphatidylethanolamine (DOPE/DOPG 7:3) further decreased the yield of tKcsA to ~40% (Fig. 3B, lane 3, Fig. 1S, lane 2) and led to the formation of the large particles (14–25 nm) containing tKcsA and MSP^- molecules (Fig 3A, trace 3). The reconstructed KcsA/LPN/DMPG complexes contained almost equal amounts of the tetrameric and monomeric channel (Fig. 3B, lane 7, Fig. 1S, lane 10). In the case of KcsA/LPN/DMPC the yield of the complex formation was extremely low and did

Table 1
Efficiency of the KcsA refolding depends on the lipid composition of LPN.

Lipid composition of LPN	DOPE/DOPG(7:3)	POPC	POPC/DOPG(7:3)	DMPC	DMPG
Formation of KcsA/LPN complexes[a]	−	+	+	−	+
Yield of tKcsA folding, %[b]	31/50	90/73	49/61	7/17	35/60
Residual fraction of mKcsA, %[b]	n.o.[c]/11	n.o.[c]/7	n.o.[c]/9	n.o.[c]/3	20/40

Table note:
[a] The ability of the tested lipid compositions to support the formation of KcsA/LPN complexes was qualitatively determined by size exclusion chromatography. "+" means that the KcsA/LPN complexes with diameters in a range 9–11 nm were formed. "−" means either very low efficiency of the complex formation or formation of large particles significantly exceeding the expected nanodisc diameter.
[b] The amounts of tKcsA and mKcsA within the reconstructed LPNs after Ni^{2+}-affinity purification were qualitatively determined by densitometry analysis of the Coomassie-stained SDS-PAGE gels presented in the Fig. 3B (lanes 3–7) and Fig. S1 (lanes 2, 4, 6, 8, 10). In each case the two values are given. The first value corresponds to the experiments where assembly and purification of KcsA/LPN complexes were done in the presence of 10 mM KCl (Fig. 3B). The second value corresponds to the experiments conducted in the absence of explicitly added potassium ions (Fig. S1). The reported percentages are given relative to the initial amount of tKcsA used for denaturation/folding (Fig. 3A, lane 8 and Fig. S1, lane 11, respectively). A relative error in the measurements doesn't exceed 15%.
[c] n.o. indicates that the mKcsA band was not observed by SDS-PAGE (the amount of mKcsA is less than 5% from the initial protein amount).

not exceed 20% (Fig 3B, lane 6, Fig. 1S, lane 8). Interestingly, with the exception of the LPN/DMPG complexes the residual content of mKcsA in the obtained preparations did not exceed 11% from the initial amount of tKcsA used for denaturation/folding (Table 1). Thus, similarly to the situation observed for ESR, the overall yield of the KcsA folding was primarily restricted by the efficiency of the protein encapsulation into nanodiscs.

The low yield of the KcsA/LPN/DMPC complex formation was probably conditioned by the protein precipitation or association with the Biobeads™ adsorbent during the nanodisc assembly (see Fig. S2). Indeed the formation of the precipitate containing mKcsA was observed after incubation of the mKcsA/MSP^{-}/DMPC/SDS/cholate mixture with the adsorbent in the several independent experiments. In this case the "empty" LPN/DMPC complexes not containing KcsA were also formed (data not shown). These "empty" LPNs were effectively filtered out by the Ni^{2+}-affinity chromatography and were not detected by the subsequent SEC analysis (Fig. 3A, trace 6).

The incomplete removal of the harsh detergent (SDS) could be one of the probable origins of the mKcsA precipitation during the nanodisc assembly. To investigate the influence of the SDS on the process of the nanodisc assembly we conducted the control experiments with the "empty" LPNs. The nanodiscs without encapsulated IMP were formed from the mixture of MSP^{+}, lipids, SDS and sodium cholate. The employed experimental protocol was similar to the one used for reconstruction of the KcsA/LPN complexes. The identical sample volume, lipid and detergent concentrations, added adsorbent amount, incubation time and temperature were used. Two lipid compositions POPC and DMPC (where KcsA losses during the LPN reconstruction were minimal and maximal, respectively) were assayed. In both tested cases the incubation with Biobeads™ induced the formation of the LPN particles having the characteristic diameter ~10 nm. The obtained SEC profiles (Fig. S3) were almost identical to the profiles of the nanodiscs assembled using conventional protocol, where only one detergent (sodium cholate) is used. NMR analysis of the obtained preparations (Fig. S4, S5, and S6) revealed the significant decrease in the concentration of both detergents (Table S1), however the removal of sodium cholate was more efficient. The residual detergent content was approximately twice higher in the LPN/DMPC sample (~0.7 mM of SDS and ~0.2 mM of sodium cholate) than in LPN/POPC (~0.35 and ~0.08 mM, respectively). Ni^{2+}-affinity purification led to the further decrease of the detergent concentration in the obtained LPN samples (Table S1).

4. Discussion

Large-scale production in a misfolded and/or aggregated form coupled with the *in vitro* folding is considered as a promising alternative to the membrane-targeted expression of IMPs [6,7]. The bacterial expression in a form of inclusion bodies or CF synthesis in a form of precipitate could provide the necessary amounts of the misfolded proteins [4,6,8,9]. The main bottleneck of this strategy is to establish an efficient refolding protocol [6,7,15,18]. As it was already mentioned, the universal and generally applicable protocols for the *in vitro* folding of the helical polytopic and multimeric IMPs are presently unavailable [10,11]. Nevertheless the general strategy of the refolding was delineated in several works (for review see [6,7,12]). The proposed methods are indirectly related to the two-stage model of the IMP folding [34]. In line with this model the successful refolding methods usually involve two general steps. Initially, a helical IMP is solubilized in a "denaturing membrane mimetic", e.g. organic solvent with low polarity or harsh detergent. This step should lead to the formation of the monomeric partially denatured IMP. Please note that this protein state, as opposed to the unfolded state of globular (water soluble) proteins in chaotropic agents, is characterized by the relatively large content of the helical secondary structure [10–13,16,26,33]. On the final step of the refolding procedure the IMP is transferred into the milder membrane mimicking medium (e.g. lipid vesicles, mild detergents, lipid/detergents mixtures, etc.) that enforces the formation of the correct secondary, tertiary, and quaternary structures [14].

Here using examples of the bacteriorhodopsin ESR (7TM topology) and full-length homotetrameric K^{+} channel KcsA (4×2TM topology) we provided the evidences that the last stage of the refolding protocol could be coupled with the encapsulation of an IMP into the lipid–protein particles also known as nanodiscs. The major advantages of the nanodiscs over conventionally used membrane mimetics are the relatively small size, controlled stoichiometry, and enhanced stability of the IMP/LPN complexes [9,19–22,25]. It should be noted that previously LPNs were successfully applied for the encapsulation of the natively folded proteins extracted from the cellular membranes under non-denaturing conditions by the mild detergents [20–22,25]. The application of LPNs for co-translational folding of the IMPs during the CF synthesis was also reported [9,35,36]. The results presented here further expand the possible applications of the nanodisc technology. We showed for the first time that IMP/LPN complexes can be successfully reconstructed from a partially denatured monomeric protein solubilized in a harsh detergent (SDS), and the formation of the IMP/LPN complexes induces the folding of protein TM domains (see below).

The bacteriorhodopsins of *Halobacteria* represent a rare example of IMPs for which the refolding protocols with almost 100% efficiency were developed [16,17,26,27]. For example, the *H. salinarum* bacteriorhodopsin partially denatured by SDS can be folded with a high yield in the environment of the DMPC/CHAPS bicelles [16,26,27]. The object of the present study bacteriorhodopsin ESR from gram-positive bacteria *Exiguobacterium sibiricum* also undergoes partial unfolding in the SDS solution. This process is accompanied by the dissociation of the retinal moiety (Fig. 2BF) and moderate changes in the protein secondary structure (Fig. 2G). The spontaneous folding of ESR was observed upon the addition of the DMPC/cholate mixture to the SDS denatured protein. Thus, to directly investigate the applicability of the nanodisc-based

refolding strategy we were forced to exclude commonly used sodium cholate from the reaction of the ESR/LPN reconstruction and use SDS as the sole detergent component of the reaction mixture. In spite of the changes in the protocol, the successful incorporation of ESR into LPN/DMPC and LPN/DMPG was achieved. Obtained ESR/LPN complexes in both cases contained about 80% of the spectroscopically active protein indicating the proper folding of the 7-helical TM bundle which surrounds the retinal binding pocket. The amount of the folded protein roughly corresponds to the efficiency of the co-translational ESR folding (80–90%) observed during CF synthesis in the presence of DMPC and DMPG LPNs [9]. Interestingly, the overall yield of the ESR folding was primarily restricted by the efficiency of the protein encapsulation into LPNs and dramatically depended on the lipid composition of the nanodiscs. The largest yield (~60%) was observed in LPNs containing anionic lipids (DMPG) and was twice lower in zwitterionic lipids (DMPC).

Several approaches for the refolding of the homotetrameric tKcsA channel from the partially denatured mKcsA monomers were previously described [18,37,38]. It was shown that the folding efficiency depends on the properties of the used denaturant and refolding medium. For example the incorporation of SDS denatured mKcsA into differently charged lipid vesicles led to the formation of natively folded tKcsA with a yield of about 30% [18]. Contrary to that, the mixture of DOPE/DOPG lipids in the form of the vesicles or mixed micelles with the mild detergent DDM provided an almost qualitative (>90%) tKcsA refolding from the TFE denatured state [37,38]. Moreover, an anionic lipid mixture (DOPE/DOPG 7:3) containing a large proportion of phosphatidylethanolamine, a lipid with a negative spontaneous curvature, was reported as optimal for the KcsA renaturation *in vitro* [37,38].

Here we observed that the treatment with the strong acid followed by the solubilization in SDS induces the dissociation of the homotetrameric tKcsA channel into the monomers (Fig. 3B). The incorporation of the partially denatured mKcsA monomers into the nanodiscs resulted in the reassembly of the homotetrameric channel (Fig. 3B, Fig. S1). According to the structural data, the tetramerization of KscA is mostly dominated by the interactions within the 8-helical TM domain [28–32]. Referring to the results of the previous folding studies [18,37], we can conclude that the observation of the tKcsA band on the SDS-PAGE gels (Fig. 3B and 1S) confirms the correct folding of the TM domain. However, the full-length KcsA channel also involves the cytoplasmic domain formed from the *N*- and *C*-terminal fragments of the individual subunits. Crystallographic [29] and EPR spectroscopy [32] studies of the natively folded tetrameric channel revealed that the *N*-terminal helical fragments of each subunit are anchored at the membrane–water interface and the *C*-terminal fragments form the extramembrane 4-helical bundle (see Fig. 1). The recent denaturation/folding study of the truncated KcsA variants revealed that the *N*- and *C*-terminal fragments could significantly influence the homotetramer stability and efficiency of the channel refolding from the monomeric state [39]. The presently obtained data do not give any information about the structural state (folded/unfolded) of the extra-membrane KcsA domain. Taking in mind the numerous examples of the nanodisc usage for stabilization and studies of the peripheral membrane proteins (e.g. cytochromes P450, cytochrome P450 reductase [40], and blood-clotting protease TF:FVIIa [41], etc.) we could speculate that the lipid bilayer fragment enclosed within the LPN particle is able to adequately mimic not only the hydrophobic region of the membrane but also the membrane–water interface. Thus the nanodiscs could provide a unique environment for simultaneous folding of the transmembrane and extramembrane domains of IMPs.

The efficiency of tKcsA refolding demonstrated pronounced dependence on the lipid composition of nanodiscs (Table. 1). The largest tKcsA yield (70–90%), comparable with the results obtained using classical membrane mimetics [37,38], was observed in the zwitterionic unsaturated lipid (POPC). Most surprisingly, the efficiency of tKcsA folding using DOPE/DOPG mixture was quite low (30–50%) and was accompanied by the formation of the large-sized particles (Table 1 and Fig. 3A, lane 3). These particles having a diameter of ~20 nm contain tKcsA and MSP^{-} molecules and probably represent the "fused" or "remodeled" lipoproteins [42]. It should be noted that the "fusion" of the nanodiscs composed from the unsaturated lipids was previously observed during the co-translational incorporation of CF synthesized IMPs [9]. The obtained data are also consistent with the results of our previous work where the effective reconstruction of natively folded tetrameric KcsA into LPNs containing DMPC and POPC, but not DOPE/DOPG, was observed [25]. The inefficiency of the LPN formation from the DOPG/DOPE mixture can be explained by the inability of MSP to stabilize the lipid bilayer with the large negative curvature strain induced by DOPE.

The lowest efficiency of the KcsA/LPN reconstruction and tKcsA folding (<20%) was observed in the zwitterionic saturated lipid (DMPC). This effect was caused by the mKcsA precipitation during the nanodisc assembly. The observed protein precipitation was quite unexpected as the successful reconstruction of the tKcsA/LPN/DMPC complexes had been reported previously [25]. With the exception of the initial KscA state, the almost identical protocols of the nanodisc assembly were employed in both cases. The tetrameric form of the channel in DDM solution and the monomeric protein solubilized in SDS were used in the previous and current works, respectively. The control experiments with "empty" LPN/DMPC and LPN/POPC (containing only MSP and lipid molecules) revealed that the usage of the harsh detergent SDS does not interfere with the nanodisc assembly (Fig. S3). At the same time, the residual concentration of SDS was approximately twice higher in the LPN/DMPC sample than in the LPN/POPC one (Table S1). It should be noted that the determined concentrations (0.7 and 0.35 mM, respectively) were significantly lower than the critical micelle concentration of SDS (6 mM) and corresponded to only few detergent molecules (<6) per one nanodisc. In spite of this, we could assume that the delayed or incomplete SDS removal during the process of the LPN/DMPC reconstruction is at least partially responsible for the observed mKcsA precipitation.

SEC analysis revealed the presence of the size heterogeneity of some of the obtained IMP/LPN and "empty" LPN preparations (Fig. 3A and 3S). This is not surprising as these IMP/LPN samples indeed represent the heterogeneous mixtures containing nanodisc complexes with the folded and unfolded proteins. In the case of KcsA the situation is the most complicated as the LPN complexes with the different KcsA stoichiometries (monomer, tetramer, tetramer and monomer, tetramer and two monomers, etc.) are probably formed. On the other hand the reconstructed high-density lipoproteins or "empty" nanodiscs frequently represent the mixtures of the differently sized particles which could be detected by SEC, native PAGE, AFM and other techniques [42–44]. The production of the monodisperse nanodisc preparations requires a careful optimization of the self-assembly protocol [19,25,42]. Probably the IMP/MSP/lipid molar ratios and incubation temperature should be optimized in the each particular case. In the present work to obtain the self-consistent results, we used identical parameters of the nanodisc assembly in each of the experiments. For example, the equal temperature (25 °C) was used for the LPN reconstruction from saturated and unsaturated lipids characterized by different phase transition temperatures. We suggest that the presence of LPNs containing the unfolded proteins and employment of the non-optimal protocols of the nanodisc assembly are responsible for the observed size heterogeneity.

The initial structural state of an aggregated/misfolded helical IMP could significantly depend on the used method of the recombinant production. Precipitates produced during CF synthesis in the absence of membrane mimicking components probably contain IMPs with a significant level of the already formed helical secondary structure [45]. As a consequence IMPs could be easily solubilized from the CF precipitate by the moderately harsh detergents, like DPC and LMPG [8,45]. Contrary to that, the bacterial inclusion bodies probably contain more strongly aggregated proteins, and in this case the IMP solubilization requires the application of harsh detergents, like SDS and sodium lauroyl sarcosinate.

Although the information about the IMP state within the inclusion bodies is presently unavailable, it should be noted that the β-sheet-rich amyloid-like structures were detected in the case of some globular proteins [46]. The precipitation of IMPs by trichloroacetic acid used in this work probably results in the protein samples with the structural properties similar to the CF precipitate. Previously it was shown that an acid precipitated IMP could be easily resolubilized by the moderately harsh detergents (DPC, LMPG) but not by mild detergents (e.g. DDM) [22]. In spite of the differences in the initial protein state we propose that the nanodisc-based refolding strategy also could be applied for the *in vitro* folding of IMPs produced in the form of inclusion bodies. In this case, the solubilization and "monomerization" of the target protein should be achieved before the reconstruction of the IMP/LPN complexes (see Fig. 1).

5. Conclusions

In summary, for the first time we showed that the lipid–protein nanodiscs can serve as a suitable medium for the *in vitro* folding of recombinant membrane proteins. A partially denatured IMP solubilized in a harsh detergent (like SDS) could be simply mixed with the apolipoprotein (MSP) and lipids. Detergent removal results in the spontaneous formation of LPNs containing the IMP with the folded TM domain. The efficiency of the proposed approach depends on the properties of the LPN membrane and the optimization of lipid composition is required to achieve the efficient folding. The application of the lipid–protein nanodiscs as the medium for the *in vitro* folding of membrane proteins opens new perspectives in the structural–functional studies of these pharmacologically important biomolecules.

Acknowledgements

The work was supported by the Russian Foundation for Basic Research (grants 10-04-01752, 12-04-01712, and 12-04-31485), the Russian Federal Target Program "Scientific and Science-Educational Personnel of Innovative Russia" (Projects 8789, and 8268), and the Russian Academy of Sciences (Program "Molecular and Cellular Biology").

Appendix A. Supplementary

Supplementary data to this article can be found online at http://dx.doi.org/10.1016/j.bbamem.2012.11.005.

References

[1] In: K.H. Lundstrom (Ed.), Structural Genomics on Membrane Proteins, CRC Press, 2006.
[2] E. Wallin, G. von Heijne, Genome-wide analysis of integral membrane proteins from eubacterial, archaean, and eukaryotic organisms, Protein Sci. 7 (1998) 1029–1038.
[3] J.P. Overington, B. Al Lazikani, A.L. Hopkins, How many drug targets are there? Nat. Rev. Drug Discov. 5 (2006) 993–996.
[4] E.C. McCusker, S.E. Bane, M.A. O'Malley, A.S. Robinson, Heterologous GPCR expression: a bottleneck to obtaining crystal structures, Biotechnol. Prog. 23 (2007) 540–547.
[5] F. Junge, B. Schneider, S. Reckel, D. Schwarz, V. Dötsch, F. Bernhard, Large-scale production of functional membrane proteins, Cell. Mol. Life Sci. 65 (2008) 1729–1755.
[6] H. Kiefer, *In vitro* folding of alpha-helical membrane proteins, Biochim. Biophys. Acta 1610 (2003) 57–62.
[7] J.L. Baneres, J.L. Popot, B. Mouillac, New advances in production and functional folding of G-protein-coupled receptors, Trends Biotechnol. 29 (2011) 314–322.
[8] F. Junge, S. Haberstock, C. Roos, S. Stefer, D. Proverbio, V. Dötsch, F. Bernhard, Advances in cell-free protein synthesis for the functional and structural analysis of membrane proteins, New Biotechnol. 28 (2011) 262–271.
[9] E.N. Lyukmanova, Z.O. Shenkarev, N.F. Khabibullina, G.S. Kopeina, M.A. Shulepko, A.S. Paramonov, K.S. Mineev, R.V. Tikhonov, L.N. Shingarova, L.E. Petrovskaya, D.A. Dolgikh, A.S. Arseniev, M.P. Kirpichnikov, Lipid–protein nanodiscs for cell-free production of integral membrane proteins in a soluble and folded state: comparison with detergent micelles, bicelles and liposomes, Biochim. Biophys. Acta 1818 (2012) 349–358.
[10] P.J. Booth, P. Curnow, Membrane proteins shape up: understanding *in vitro* folding, Curr. Opin. Struct. Biol. 16 (2006) 480–488.
[11] S. Fiedler, J. Broecker, S. Keller, Protein folding in membranes, Cell. Mol. Life Sci. 67 (2010) 1779–1798.
[12] A.M. Stanley, K.G. Fleming, The process of folding proteins into membranes: challenges and progress, Arch. Biochem. Biophys. 469 (2008) 46–66.
[13] V. Krishnamani, B.G. Hegde, R. Langen, J.K. Lanyi, Secondary and tertiary structure of bacteriorhodopsin in the SDS denatured state, Biochemistry 51 (2012) 1051–1060.
[14] V. Krishnamani, J.K. Lanyi, Structural changes in bacteriorhodopsin during *in vitro* refolding from a partially denatured state, Biophys. J. 100 (2011) 1559–1567.
[15] M. Bosse, L. Thomas, R. Hassert, A.G. Beck-Sickinger, D. Huster, P. Schmidt, Assessment of a fully active class A G protein-coupled receptor isolated from *in vitro* folding, Biochemistry 50 (2011) 9817–9825.
[16] K.S. Huang, H. Bayley, M.J. Liao, E. London, H.G. Khorana, Refolding of an integral membrane protein. Denaturation, renaturation and reconstitution of intact bacteriorhodopsin and two proteolytic fragments, J. Biol. Chem. 256 (1981) 3802–3809.
[17] S.J. Allen, A.R. Curran, R.H. Templer, W. Meijberg, P.J. Booth, Controlling the folding efficiency of an integral membrane protein, J. Mol. Biol. 342 (2004) 1293–1304.
[18] F.I. Valiyaveetil, Y. Zhou, R. MacKinnon, Lipids in the structure, folding, and function of the KcsA K+ channel, Biochemistry 41 (2002) 10771–10777.
[19] I.G. Denisov, Y.V. Grinkova, A.A. Lazarides, S.G. Sligar, Directed self-assembly of monodisperse phospholipid bilayer nanodiscs with controlled size, J. Am. Chem. Soc. 126 (2004) 3477–3487.
[20] A. Nath, W.M. Atkins, S.G. Sligar, Applications of phospholipid bilayer nanodiscs in the study of membranes and membrane proteins, Biochemistry 46 (2007) 2059–2069.
[21] T.H. Bayburt, S.G. Sligar, Membrane protein assembly into nanodiscs, FEBS Lett. 584 (2010) 1721–1727.
[22] Z.O. Shenkarev, E.N. Lyukmanova, A.S. Paramonov, L.N. Shingarova, V.V. Chupin, M.P. Kirpichnikov, M.J. Blommers, A.S. Arseniev, Lipid–protein nanodiscs as reference medium in detergent screening for high-resolution NMR studies of integral membrane proteins, J. Am. Chem. Soc. 132 (2010) 5628–5629.
[23] L.E. Petrovskaya, E.P. Lukashev, V.V. Chupin, S.V. Sychev, E.N. Lyukmanova, E.A. Kryukova, R.H. Ziganshin, E.V. Spirina, E.M. Rivkina, R.A. Khatypov, L.G. Erokhina, D.A. Gilichinsky, V.A. Shuvalov, M.P. Kirpichnikov, Predicted bacteriorhodopsin from *Exiguobacterium sibiricum* is a functional proton pump, FEBS Lett. 584 (2010) 4193–4196.
[24] L. Heginbotham, E. Odessey, C. Miller, Tetrameric stoichiometry of a prokaryotic K+ channel, Biochemistry 36 (1997) 10335–10342.
[25] Z.O. Shenkarev, E.N. Lyukmanova, O.I. Solozhenkin, I.E. Gagnidze, O.V. Nekrasova, V.V. Chupin, A.A. Tagaev, Z.A. Yakimenko, T.V. Ovchinnikova, M.P. Kirpichnikov, A.S. Arseniev, Lipid–protein nanodiscs: possible application in high-resolution NMR investigations of membrane proteins and membrane-active peptides, Biochemistry (Mosc) 74 (2009) 756–765.
[26] P. Curnow, P.J. Booth, Combined kinetic and thermodynamic analysis of alpha-helical membrane protein unfolding, Proc. Natl. Acad. Sci. U. S. A. 104 (2007) 18970–18975.
[27] P.J. Booth, S.L. Flitsch, L.J. Stern, D.A. Greenhalgh, P.S. Kim, H.G. Khorana, Intermediates in the folding of the membrane protein bacteriorhodopsin, Nat. Struct. Biol. 2 (1995) 139–143.
[28] D.A. Doyle, C.J. Morais, R.A. Pfuetzner, A. Kuo, J.M. Gulbis, S.L. Cohen, B.T. Chait, R. MacKinnon, The structure of the potassium channel: molecular basis of K+ conduction and selectivity, Science 280 (1998) 69–77.
[29] S. Uysal, V. Vásquez, V. Tereshko, K. Esaki, F.A. Fellouse, S.S. Sidhu, S. Koide, E. Perozo, A. Kossiakoff, Crystal structure of full-length KcsA in its closed conformation, Proc. Natl. Acad. Sci. U. S. A. 106 (2009) 6644–6649.
[30] J.H. Chill, J.M. Louis, C. Miller, A. Bax, NMR study of the tetrameric KcsA potassium channel in detergent micelles, Protein Sci. 15 (2006) 684–698.
[31] K.A. Baker, C. Tzitzilonis, W. Kwiatkowski, S. Choe, R. Riek, Conformational dynamics of the KcsA potassium channel governs gating properties, Nat. Struct. Mol. Biol. 14 (2007) 1089–1095.
[32] D.M. Cortes, L.G. Cuello, E. Perozo, Molecular architecture of full-length KcsA: role of cytoplasmic domains in ion permeation and activation gating, J. Gen. Physiol. 117 (2001) 165–180.
[33] J.H. Chill, J.M. Louis, F. Delaglio, A. Bax, Local and global structure of the monomeric subunit of the potassium channel KcsA probed by NMR, Biochim. Biophys. Acta 1768 (2007) 3260–3270.
[34] J.L. Popot, D.M. Engelman, Membrane protein folding and oligomerization: the two-stage model, Biochemistry 29 (1990) 4031–4037.
[35] F. Katzen, J.E. Fletcher, J.P. Yang, D. Kang, T.C. Peterson, J.A. Cappuccio, C.D. Blanchette, T. Sulchek, B.A. Chromy, P.D. Hoeprich, M.A. Coleman, W. Kudlicki, Insertion of membrane proteins into discoidal membranes using a cell-free protein expression approach, J. Proteome Res. 7 (2008) 3535–3542.
[36] J.A. Cappuccio, C.D. Blanchette, T.A. Sulchek, E.S. Arroyo, J.M. Kralj, A.K. Hinz, E.A. Kuhn, B.A. Chromy, B.W. Segelke, K.J. Rothschild, J.E. Fletcher, F. Katzen, T.C. Peterson, W.A. Kudlicki, G. Bench, P.D. Hoeprich, M.A. Coleman, Cell-free co-expression of functional membrane proteins and apolipoprotein, forming soluble nanolipoprotein particles, Mol. Cell Proteomics 7 (2008) 2246–2253.
[37] F.N. Barrera, M.L. Renart, J.A. Poveda, B. de Kruijff, J.A. Killian, J.M. González-Ros, Protein self-assembly and lipid binding in the folding of the potassium channel KcsA, Biochemistry 47 (2008) 2123–2133.
[38] V.V. Chupin, O.V. Nekrasova, M.P. Kirpichnikov, A.S. Arseniev, Method of producing renatured membrane proteins, Patent of Russian Federation #2306319 from 07.12.2005.
[39] M. Raja, The role of extramembranous cytoplasmic termini in assembly and stability of the tetrameric K(+)-channel KcsA, J. Membr. Biol. 235 (2010) 51–61.
[40] I.G. Denisov, S.G. Sligar, Cytochromes P450 in nanodiscs, Biochim. Biophys. Acta 1814 (2011) 223–229.

[41] A.W. Shaw, V.S. Pureza, S.G. Sligar, J.H. Morrissey, The local phospholipid environment modulates the activation of blood clotting, J. Biol. Chem. 282 (2007) 6556–6563.
[42] N.O. Fischer, C.D. Blanchette, B.W. Segelke, M. Corzett, B.A. Chromy, E.A. Kuhn, G. Bench, P.D. Hoeprich, Isolation, characterization, and stability of discretely-sized nanolipoprotein particles assembled with apolipophorin-III, PLoS One 5 (2010) e11643.
[43] B.A. Chromy, E. Arroyo, C.D. Blanchette, G. Bench, H. Benner, J.A. Cappuccio, M.A. Coleman, P.T. Henderson, A.K. Hinz, E.A. Kuhn, J.B. Pesavento, B.W. Segelke, T.A. Sulchek, T. Tarasow, V.L. Walsworth, P.D. Hoeprich, Different apolipoproteins impact nanolipoprotein particle formation, J. Am. Chem. Soc. 129 (2007) 14348–14354.
[44] C.D. Blanchette, R. Law, W.H. Benner, J.B. Pesavento, J.A. Cappuccio, V. Walsworth, E.A. Kuhn, M. Corzett, B.A. Chromy, B.W. Segelke, M.A. Coleman, G. Bench, P.D. Hoeprich, T.A. Sulchek, Quantifying size distributions of nanolipoprotein particles with single-particle analysis and molecular dynamic simulations, J. Lipid Res. 49 (2008) 1420–1430.
[45] I. Maslennikov, C. Klammt, E. Hwang, G. Kefala, M. Okamura, L. Esquivies, K. Mörs, C. Glaubitz, W. Kwiatkowski, Y.H. Jeon, S. Choe, Membrane domain structures of three classes of histidine kinase receptors by cell-free expression and rapid NMR analysis, Proc. Natl. Acad. Sci. U. S. A. 107 (2010) 10902–10907.
[46] L. Wang, S.K. Maji, M.R. Sawaya, D. Eisenberg, R. Riek, Bacterial inclusion bodies contain amyloid-like structure, PLoS Biol. 6 (2008) e195.